International Journal of Thermophysics, Vol. 28, No. 5, October 2007 (© 2007)
DOI: 10.1007/s10765-007-0165-3

Simultaneous Estimation of Thermal Properties of Living Tissue Using Noninvasive Method[1]

Kai Yue,[2,3] Xinxin Zhang,[2,3] and Fan Yu[2]

A new noninvasive measurement method is presented for simultaneous estimation of the key thermal properties of cylindrical living tissue. This method is based on heating of the surface of a cylinder and measuring surface temperatures at three points on the cylinder. Numerical calculations and theoretical analysis for the corresponding two-dimensional model are carried out. The results have demonstrated the feasibility of the proposed method. The selection, crossover, and mutation operators of a new real-coded genetic algorithm (GA) are designed in this paper to solve the problem of parameter optimization. Then, a set of simulations are performed to verify the effectiveness of the proposed method as well as to optimize the design of the experiments. Finally, a series of experiments is performed to measure the thermal parameters of the human forearm. The experimental results indicate that the obtained parameters, such as the thermal conductivity, blood perfusion, and volumetric heat capacity, are within the range of reference values. The proposed method is easy to implement in practical applications.

KEY WORDS: bioheat transfer; blood perfusion; genetic algorithm; heat capacity; noninvasive measurement; thermal conductivity.

1. INTRODUCTION

An understanding of heat-transfer mechanisms in living tissue requires an accurate knowledge of the thermal properties of biological materials, which are characterized by thermal parameters such as thermal

[1] Paper presented at the Seventeenth European Conference on Thermophysical Properties, September 5–8, 2005, Bratislava, Slovak Republic.

[2] Department of Thermal Engineering, University of Science and Technology Beijing, Beijing 100083, P.R. China.

[3] To whom correspondence should be addressed. E-mail: xxzhang@ustb.edu.cn or yuekai@me.ustb.edu.cn

conductivity, thermal diffusivity, and blood perfusion. These parameters play an important role in both theoretical research of bioheat transfer and clinical applications including cryopreservation, disease diagnosis, hyperthermia, cancer therapy, and cryosurgery [1,2]. As a consequence, the measurement of thermal transport properties of living tissue has been one of the major research topics in the field of bioheat transfer.

Up to now, many investigators attempted to propose various methods to measure the thermal parameters of biological materials [3–5]. Among the existing techniques, the noninvasive measurement technique is the most valuable and promising for practical applications. Wei et al. [6] placed a thermal probe on the surface of human cerebra to measure blood flow. Patel et al. [7] used an inserted thermistor probe to measure effective thermal properties. Naresh et al. [8] presented an experimental technique to measure the directional thermal conductivity and thermal diffusivity of materials. Scott et al. [9] have developed a noninvasive thermal technique to obtain an estimate of local state flow by combining heat flux and temperature measurements with a model for the effect of blood perfusion on tissue thermal behavior. Reilly et al. [10] developed a new noninvasive probe to measure the blood perfusion of biological materials. Deng and Liu [11] measured the local blood perfusion based on the newly developed phase shift principle to reduce the measurement time. All these efforts have made significant contributions to the fundamental research and clinic application of bioheat transfer. However, none of the foregoing noninvasive methods can simultaneously obtain the thermal conductivity, thermal diffusivity, and blood perfusion of the tissue, which are the crucial parameters needed in bioheat-transfer research. Note that these parameters vary with different samples and under different states, which makes it harder to obtain these parameters directly. Valvano et al. [12] presented an improved technique to determine these parameters, the measurement based on the invasive insertion of a self-heated spherical thermistor probe into the perfused tissue. However, the inserted probe would affect the measured parameters themselves to some degree.

The primary objective of this paper is to develop a new noninvasive measurement technique to simultaneously determine the thermal conductivity, volumetric heat capacity, and blood perfusion of the local living tissue. A mathematical model is established for the cylindrical living tissue to study the heat transfer of human body.

2. METHOD

Due to the complexity of the bioheat-transfer equation and the existence of multiple unknown thermal parameters, it is difficult to obtain the thermal parameters of interest by directly solving the governing equation. Therefore, the inverse method has been applied to estimate the key parameters for bioheat-transfer research. The measurement of thermal parameters of living tissue is actually an inverse heat-transfer problem. Given one or more measured temperatures or heat flux variations of the measured tissue, the unknown parameters appearing in the mathematical model, i.e., the partial differential equation and its associated initial and boundary conditions, can be estimated by using an optimization method. This can be accomplished by finding the optimal measured parameters to minimize the differences between the measured temperatures and the predicted temperatures resulting from a solution of the established mathematical model.

2.1. Description of the Method

Figure 1 shows a schematic diagram of the new noninvasive inverse method proposed to simultaneously estimate the concerned thermal parameters of living tissues. A thin piece of sheet metal is wrapped around the surface of the cylindrical sample, as shown in Fig. 1a. A constant power is supplied across the ends of the sheet metal for several minutes. Thus, the measured tissue is affected by a thermal perturbation signal with a constant heat flux, which can be a step signal or a square wave signal as shown in Fig. 1b.

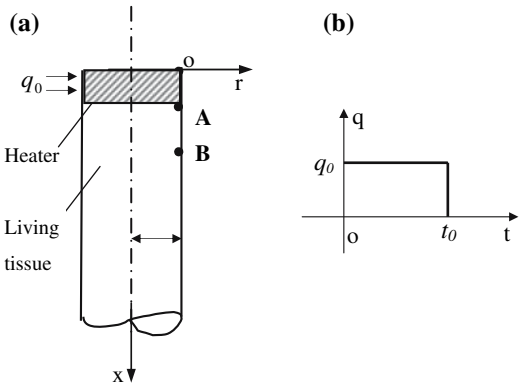

Fig. 1. (a) Schematic diagram and (b) thermal perturbation signal of the method.

Points O, A, and B are three measuring locations on the surface of the living tissue and are located along the axial direction. Due to the need for simultaneous estimations of multiple parameters, one cannot usually meet the demand to obtain the practical temperature variations from just one measuring site. Thus, we select as many available measuring points as possible. The selection of points O, A, and B is based on the consideration that the temperature variations of the measured points should represent and distinctively reflect the effects of a thermal perturbation signal on the measured tissue. This issue will be further discussed in the following sections. The measured temperature variations at each of the measuring points O, A, and B can be expressed as follows:

$$T_i(\beta, t)\ \{i = \mathrm{O}, \mathrm{A}, \mathrm{B} \qquad \beta = (\beta_1, \beta_2, \ldots, \beta_p)^T\} \tag{1}$$

where β is the parameter vector, including the estimated parameters which affect the temperature responses at the measuring points, such as thermal parameters, geometrical parameters, convection heat-transfer coefficient, etc; and p is the number of estimated parameters. The other data needed to solve the inverse problem are the predicted temperature variations resulting from the established thermal model.

2.2. Thermal Model

Thermal energy transport in living tissue is a complex process including conduction, convection, radiation, interior metabolism, evaporation, phase change, and inherent temperature regulation. Moreover, the remarkable effect of blood perfusion on the temperature field varies among the different tissues and organs. Consequently, it is very difficult to build generally applicable models to precisely describe the heat-transfer process. Of all the applied bioheat equations, it has been demonstrated that the equation proposed by Pennes in 1948 is the most successfully used bioheat-transfer equation although some of the assumptions are not valid [13]. Based on Pennes' equation [14], the mathematical model is established to describe the heat-transfer process of the living tissue of interest in this paper. Thus, the governing equation in two-dimensional cylindrical coordinates can be expressed as follows:

$$(\rho c)_{\mathrm{t}} \frac{\partial T}{\partial t} = k\left[\frac{\partial^2 T}{\partial x^2} + \frac{1}{r}\frac{\partial}{\partial r}\left(r\frac{\partial T}{\partial r}\right)\right] + w_{\mathrm{b}} c_{\mathrm{b}}(T_{\mathrm{a}} - T) + q_{\mathrm{m}} \tag{2}$$

where ρ, c, k denote the density, specific heat, and thermal conductivity of the tissue, respectively; w_{b} denotes the blood perfusion rate per unit volume; c_{b} is the specific heat of blood; q_{m} is the metabolic heat generation

per unit volume; T_a represents the constant temperature of arterial blood (37°C); and T is the tissue temperature. In this model, it is assumed that the blood perfusion effect is homogeneous and isotropic in the given local tissue and the temperature of the venous blood is assumed equal to that of the local living tissue.

In accordance with the presented measurement method, the boundary conditions can be described as follows:

$$x = 0,\ 0 < r < R,\ \frac{\partial T}{\partial x} = 0; \tag{3a}$$

$$x = L,\ 0 < r < R,\ \frac{\partial T}{\partial x} = 0; \tag{3b}$$

$$r = 0,\ 0 \le x \le L,\ \frac{\partial T}{\partial r} = 0; \tag{3c}$$

$$r = R, \begin{cases} 0 \le x \le l & \begin{cases} 0 < t \le t_0, -k\frac{\partial T}{\partial r} = q_0 \\ t > t_0,\ \frac{\partial T}{\partial r} = 0 \end{cases} \\ l < x \le L,\ -k\frac{\partial T}{\partial r} = h_A(T_- T_\infty) \end{cases} \tag{3d}$$

where q_0 is the square-wave heat flux generated by the electric heater; h_A is the heat-transfer coefficient, which accounts for the effects of heat convection and radiation heat transfer on the surface of the living tissue; T_∞ is the ambient temperature; R is the radius of the cylinder; L is the length of the cylinder; and t_0 represents the time when the power is turned off. In addition, the initial condition is set as the predicted temperature field of the corresponding steady-state model in order to agree with the practical temperature distribution of the living tissue.

It is difficult to obtain the analytical solution of the established two-dimensional mathematical model. Therefore, the numerical method is applied to solve the governing equation. The initial temperature field is set as the calculated results of the steady-state mathematical model. The predicted temperature variation can be written as $T_i(\widehat{\beta}, t)$, where the parameter vector $\widehat{\beta}$ includes the set values of the thermal parameters needed to be estimated in the thermal model. With the measured temperatures $T_i(\beta, t)$ and the predicted temperatures $T_i(\widehat{\beta}, t)$, the concerned thermal parameters of the cylindrical living tissue can be estimated by using the applicable optimization method.

2.3. Analysis of the Thermal Model

In order to validate the availability and feasibility of the proposed method and to optimize the design of the measurement method, the corresponding numerical calculations and sensitivity analysis have been carried out. Herein, the typical thermal parameters of the living tissue are set as the reference values given in Table I [15]. By solving the mathematical model, we can obtain the dynamic temperature profile along the axial direction, which is shown in Fig. 2, when the heating time is 3 min.

From Fig. 2, it can be seen that the available measuring range, which can represent the effect of the thermal perturbation signal on the heated tissue, is quite narrow. Thus, the selection of the measuring position is limited to a few points. An increase of the external heat flux can change

Table I. Reference Values Used in Theoretical Analysis

Parameters		Typical values
k	Thermal conductivity	$0.24–0.48\,W \cdot m^{-1} \cdot {}^{\circ}C^{-1}$
c_b	Specific heat of blood	$3850\,J \cdot kg^{-1} \cdot {}^{\circ}C^{-1}$
h_A	Heat transfer coefficient	$7–15\,W \cdot m^{-2} \cdot {}^{\circ}C^{-1}$
q_m	Metabolic heat generation	$0–1085\,W \cdot m^{-3}$
w_b	Blood perfusion	$1.5–3.0\,kg \cdot s^{-1} \cdot m^{-3}$
ρc	Volumetric heat capacity	$1.675 \times 10^6–3.134 \times 10^6\,J \cdot m^{-3} \cdot {}^{\circ}C^{-1}$
T_A	Arterial blood temperature	37°
q_0	External heat flux	$500\,W \cdot m^{-2}$

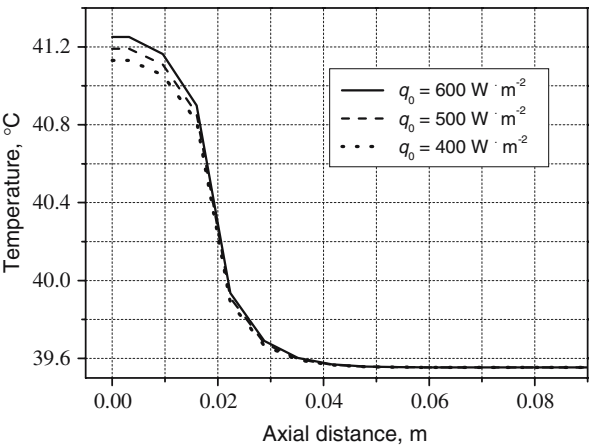

Fig. 2. Temperature variations with time and axial distance.

the temperature profiles, but cannot widen the available measuring range. The same phenomenon occurs when the width of the sheet-metal heater is changed. Upon analyzing the temperature variations along the axial direction, we find that there are three representative temperature responses in the available measuring range. Correspondingly, we select three measuring points on the surface of the model, i.e., the point O at the mid-point of the heater, point A in the region in which the temperature changes sharply, and point B in the region in which the temperature changes gently. While analyzing the effects of each parameter involved in the mathematical model on the temperature variations, we found that changes of the metabolic heat generation had little effect on the temperature distribution. Thus, an estimation of this parameter is not discussed in this paper.

To determine whether the thermal parameters of interest can be simultaneously estimated with satisfactory accuracy, the sensitivities of the temperature variations at three measuring points to the parameters of interest here are calculated. The results [16] indicate that the sensitivity coefficients of the thermal conductivity, blood perfusion, and volumetric heat capacity are relatively high. Moreover, the curve variations of the sensitivity coefficients of different thermal parameters are not exactly the same, which means that the sensitivity coefficients of the estimated thermal parameters are linearly independent. As a consequence, it is concluded that the thermal conductivity, blood perfusion, and volumetric heat capacity of the living tissue can be estimated with good precision and can be simultaneously obtained by using the proposed measurement method.

3. ESTIMATION METHOD

To solve an inverse problem, an applicable estimation method must be designed to search for the optimal solutions of the unknown parameter by minimizing the least-squares objective function. Conventional gradient-based methods have been widely and successfully used to solve general optimization problems. However, the performances of these methods require the derivative of the objective function, initial guesses of the values of the parameters of interest, and other auxiliary knowledge.

As described in previous sections, the unknown parameters in the established mathematical model include the thermal conductivity k, blood perfusion w_b, volumetric heat capacity ρc, heat-transfer coefficient h_A, and external heat flux q_0. When multiple parameters need to be simultaneously estimated, the form of the objective function in the parameter space becomes very complicated. Therefore, it is difficult to make good initial guesses to start the effective search for the global optimum as done in the conventional gradient-based method. The objective function in this

paper is defined as the sum of squares of errors between measured temperatures at three measurement locations and predicted temperatures at these locations during the heating and cooling process, which is expressed as

$$S_{\mathrm{OAB}} = \sum_{i=1}^{n} [T_{\mathrm{O}}(\beta, t) - T_{\mathrm{O}}(\widehat{\beta}, t)]^2 + \sum_{i=1}^{n} [T_{\mathrm{A}}(\beta, t) - T_{\mathrm{A}}(\widehat{\beta}, t)]^2 + \sum_{i=1}^{n} [T_{\mathrm{B}}(\beta, t) - T_{\mathrm{B}}(\widehat{\beta}, t)]^2 \Rightarrow \min \quad (i = 1, 2, \ldots, n) \tag{4}$$

where n is the number of measurements recorded over time.

Since only the numerical solutions $T_i(\widehat{\beta}, t)$ of the established mathematical model can be obtained, the derivative and the form of the objective function are difficult to analyze. In this case, a gradient-directed searching mechanism [17] usually results in nonconvergence or sub-optimal solutions. Based on a natural selection mechanism to drive biological evolution, the genetic algorithm (GA) is a global search method for solving optimization problems. The genetic algorithm repeatedly modifies a population of individual solutions. At each step, the genetic algorithm selects individuals from the current population to be parents according to the level of fitness in the problem domain, and produces the children for the next generation using operators borrowed from natural genetics. Over successive generations, the population "evolves" towards an optimal solution. This technique has been theoretically and empirically proven to provide robust searches when the objective function is characterized as being high dimensional, with real variables and many local optimal values, and when the search space is large and noisy. In this paper, a real-coded GA procedure, in which the parameters are encoded as real numbers, is developed to solve the estimation problem of thermal parameters of cylindrical living tissue.

3.1. Design of Real-Coded Genetic Algorithm

Although the GA has been proven to be a useful approach for solving a wide variety of optimization problems [18], the successful performance of a standard GA is based on the assumption that the evolution generation and population size are indefinite. Consequently, different problems usually require different designs of the GA algorithm, including selection of the coding method, determination of control variables, such as proper population size and the number of evolution generations, and selection of genetic operators, etc. In this study, a real-coded GA is designed to simultaneously estimate the thermal parameters in the mathematical model

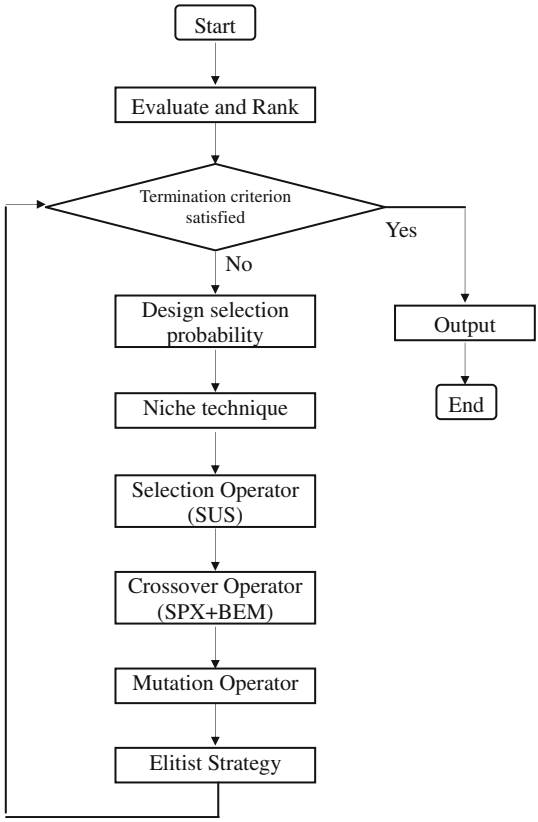

Fig. 3. Flow chart of the designed real-coded GA.

given in Eqs. (2) and (3). The flow chart is shown in Fig. 3. First, the control variables are determined and the population is initialized. The fitness value of each individual is evaluated and ranked. When the termination criterion is dissatisfied, the niche technique, the selection, crossover, mutation operators, and the elitist strategy are applied sequentially. The process will be repeated until the termination criterion is satisfied, while the global optimal solution is the output.

The thermal parameters of interest in this study are real and have wide ranges of values. The real-coded method is employed to encode the parameters because the efficiency of the GA can be increased without the need to convert chromosomes to phenotypes and there is no loss in precision by discretization to binary or other values. For convenience to evaluate the distribution of each individual in parametric space, the parameters

in the range $[a_i, b_i]$ are converted to be mapped into the range of [0,1]. The initial population of the individuals is generated by a random function to obtain the uniformly distributed individuals within the parametric search space.

The selection operator is used for the process of determining N individuals chosen for reproduction. The commonly used selection technique is the roulette wheel method, which is based simply on the fitness values of individuals and easily results in premature convergence. The stochastic universal sampling (SUS) method is employed in this paper for its minimum spread and zero bias. SUS ranks the individuals according to their fitness values and allocates the designed selection probabilities to the individuals in turn. Then, the parents are selected according to N equally spaced pointers and the mechanism of the roulette wheel method. The crossover operator for producing new chromosomes is the basic and key operator in GAs and determines the direction of search for the optimal solution. The improved simplex crossover (SPX) operator is used to generate the offspring and to expand the distribution region in this study. The offspring X_c is created as follows:

$$\begin{aligned} &X_c = X_p + R_{avg} \sum_{i=1}^{n+1} \zeta_i e_i \\ &\zeta_i \sim N(0, \sigma_\zeta^2), \quad \sigma_\zeta = c/\sqrt{n} \\ &R_{avg} = \tfrac{1}{n+1} \sum_{i=1}^{n+1} \|X_i - O\| \text{ and } O = \tfrac{1}{n+1} \sum_{i=1}^{n+1} X_i \end{aligned} \tag{5}$$

where X_p is one random individual in the simplex space formed by $n+1$ parents; O is the center of $n+1$ parents, R_{avg} is the average distance between each parent and the center O; e_i is the unit vector; ζ_i is the normally distributed random number; σ_ξ is the standard deviation; and c is a constant. In addition, the boundary extension by the mirroring (BEM) [19] method is employed to cope with the problem that the optimum of the objective function may be at the corner of the search space. The mutation operator is usually considered as the background operator to generate a new genetic gene. In this paper, mutation is randomly applied with a low probability of 0.1.

Moreover, the niche technique is applied in this study to guarantee the diversity of the population and to avoid the occurrence of premature convergence. The generational replacement is performed with a generation gap of 0.8 for the elitist strategy. The results of a number of simulations indicate that the quality of the best members of the population can be satisfied when, at most, 200 generations have been completed. Due to the probabilistic nature of GAs, the determination of the global optimal

solution requires a sufficient number of runs of the parameter estimation. In this study, the optimal estimated values of the thermal parameters are given as the average of the results obtained by carrying out the parameter estimations 30 times.

3.2. Simulations

In order to investigate the capabilities and limitations of the estimation algorithms, and to help optimize the design of experiments, a set of simulations is performed using the thermal parameters listed in Table I. To simulate the experimental data, two cases are compared with each other as shown in Fig. 4. The first one is obtained by adding the 1% random absolute error on the basis of the temperatures calculated by using the true values of the parameters. The second one is obtained by adding random errors with 0.1°C standard deviation and 0.1°C error caused by precision limitation. Of these, the second one agrees better with the practical experimental data, and is applied as the measured temperatures in the following simulations.

At first, the simultaneous estimation of five thermal parameters k, w_b, ρc, h_A, and q_0 was simulated. It was found that the temperatures calculated using the true values and the estimated values of the parameters are similar to each other when the true values are quite different from the estimated values. Figure 5 shows two groups of temperatures without the effect of random error. Herein, the true values of k, w_b, ρc, h_A, and q_0 are 0.48, 3.0, 3.134×10^6, 10, and 500, respectively, and the corresponding

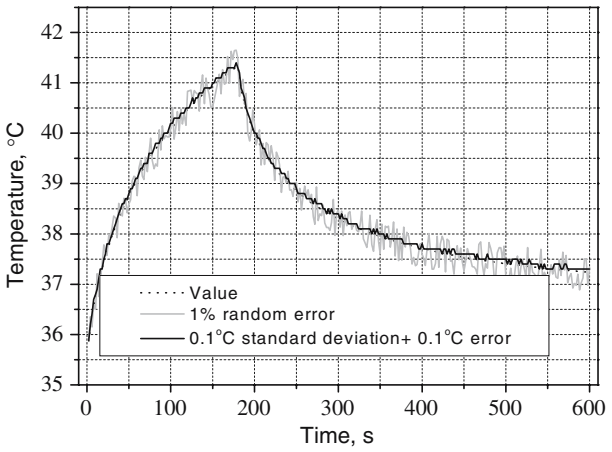

Fig. 4. Simulated experimental data.

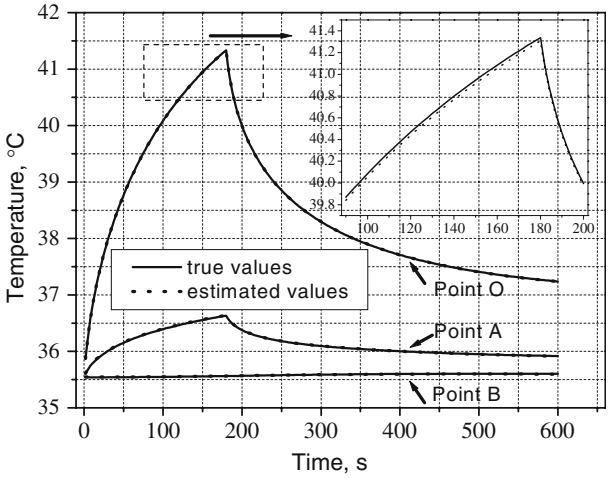

Fig. 5. Comparisons between calculated temperatures using the true values and estimated values.

estimated values are 0.447, 2.95, 3.087×10^6, 9.56, and 478.7, respectively. In this case, the maximum difference between the two groups of temperatures is only 0.03°C while the relative error of the estimated parameters can be 6.8%. This means that there is a long narrow region near the optimal solution in the parametric space, and it is very difficult to find the global optimum. These five parameters cannot be estimated simultaneously with good accuracy. Therefore, it is necessary to design the experiment to reduce the number of the parameters needed to be estimated simultaneously. In the following study, the simultaneous estimations of three and four parameters are simulated. With the simulated experimental data, the simultaneous estimations for three parameters k, w_b, ρc and k, w_b, q_0 are performed, and the results are shown in Tables II and III. Tables IV and V show, respectively, the results of the simultaneous estimations for four parameters k, w_b, ρc, h_A and k, w_b, ρc, q_0. It can be seen that three or four thermal parameters can be simultaneously estimated with good precision by using the designed real-coded GA.

In addition, the simultaneous estimation of three parameters is conducted for the case where the objective function is formed using the data measured only at point O, which is expressed as

$$S_O = \sum_{i=1}^{n} [T_O(\beta, t) - T_O(\hat{\beta}, t)]^2 \Rightarrow \min \tag{6}$$

Table II. Results of Estimations for Three Parameters k, w_b, ρc

Parameters	True values	Estimated value	Average error (%)
k ($W \cdot m^{-1} \cdot {}^\circ C^{-1}$)	0.48	0.477	−0.66
w_b ($kg \cdot s^{-1} \cdot m^{-3}$)	3.0	3.015	0.507
ρc ($J \cdot m^{-3} \cdot {}^\circ C^{-1}$)	3.134×10^6	3.15×10^6	0.407

Table III. Results of Estimations for Three Parameters k, w_b, q_0

Parameters	True values	Estimated value	Average error (%)
k ($W \cdot m^{-1} \cdot {}^\circ C^{-1}$)	0.48	0.481	0.291
w_b ($kg \cdot s^{-1} \cdot m^{-3}$)	3.0	2.9835	−0.552
q_0 ($W \cdot m^{-2}$)	500	499	0.0125

Thus, we can have good knowledge of the difference between the results obtained by using the data from three measuring points, and from one measuring point. Comparisons of results are shown in Table VI. Although the average relative errors for the case of S_O are small, they are much greater than those for the case of S_{OAB}. This phenomenon is more obvious in the simultaneous estimation of four parameters and will be further illustrated in the following experimental study.

Table IV. Results of Estimations for Four Parameters k, w_b, ρc, h_A

Parameters	True values	Estimated value	Average error (%)
k ($W \cdot m^{-1} \cdot {}^\circ C^{-1}$)	0.48	0.4807	0.0138
w_b ($kg \cdot s^{-1} \cdot m^{-3}$)	3.0	2.997	0.0923
ρc ($J \cdot m^{-3} \cdot {}^\circ C^{-1}$)	3.134×10^6	3.13×10^6	−0.0237
h_A ($W \cdot m^{-2} \cdot {}^\circ C^{-1}$)	10.023	10.026	−0.001

Table V. Results of Estimations for Four Parameters k, w_b, ρc, q_0

Parameters	True values	Estimated value	Average error (%)
k ($W \cdot m^{-1} \cdot {}^\circ C^{-1}$)	0.48	0.4814	0.283
w_b ($kg \cdot s^{-1} \cdot m^{-3}$)	3.0	2.9941	−0.198
ρc ($J \cdot m^{-3} \cdot {}^\circ C^{-1}$)	3.134×10^6	3.13×10^6	−0.231
q_0 ($W \cdot m^{-2}$)	500	499.97	−0.0053

Table VI. Comparisons of Estimations

Parameters	Average relative error (S_{OAB}) (%)	Average relative error (S_O) (%)
k ($W \cdot m^{-1} \cdot {}^\circ C^{-1}$)	−0.66%	3.3%
w_b ($kg \cdot s^{-1} \cdot m^{-3}$)	0.507%	−3.5%
ρc ($J \cdot m^{-3} \cdot {}^\circ C^{-1}$)	0.407%	−2.98%

4. EXPERIMENTS

4.1. Experimental Apparatus

Based on the foregoing numerical simulation analysis, we have designed and performed a number of experiments to verify the proposed method. The experimental study has been developed with a view to measure the thermal parameters of human forearms. The experimental apparatus is shown in Fig. 6. Wrapped around the forearm of the subject, a thin piece of sheet metal is supplied with direct and constant current by a high-precision power supply, and is used to produce the external heat flux on the measured forearm.

Upon measuring the area covered by the sheet metal and the heating power, we can determine the constant heat flux applied on the forearm. Because the junction of the thermocouple cannot be in good contact with the surface of the forearm, we chose to use three platinum resistance sensors (TRs), Pt100s with a width of 1 mm, to measure the temperature

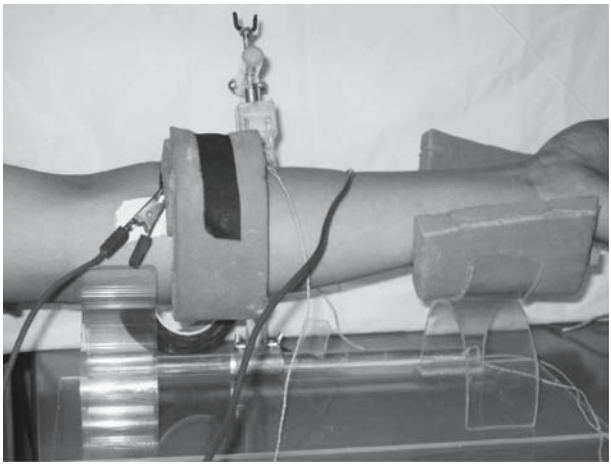

Fig. 6. Experimental apparatus.

variations at the measuring points. Therein, TR1 is located beneath the heater at point O (Fig. 1) and is insulated from the heater. A bracket is designed to adjust the position of TR2 and TR3 and fix them at point A and point B. The temperature signals measured by TRs are transferred to the computer through a data acquisition instrument. In order to reduce contact thermal resistance between the forearm and the sheet metal or the platinum resistance sensors, a silica gel material is smeared on the surface of the forearm of the subjects.

4.2. Experimental Procedure

Once the experimental apparatus is set up, the measurement of the thermal parameters of the forearm is performed while the subject is in a resting state. At first, the subject's forearm is wrapped by the sheet metal and put on the designed bracket. Then, three platinum resistance sensors are located at selected points on the surface of the forearm. The temperatures at three measuring points are steady when the whole experimental system reaches a thermal equilibrium state. Then, the power supply is turned on to generate the heat flux, and the provided heating power is measured for the determination of the heat flux. After heating for 3 min, the power supply is turned off, but the records of the temperatures are continuously monitored for 7 min. Over the duration of the entire experimental process, the temperatures are sampled every 2 s.

Using the designed GA to minimize the objective function (S_{OAB}) which measures the difference between the practically measured temperatures and the predicted temperatures by the mathematical model, four parameters, k, w_b, ρc, and h_A, are simultaneously estimated.

4.3. Experimental Results

A series of practical measurements has been performed on subjects with different physiological characteristics, such as sex, age, height, and weight of the body. The experimental results of three of the measured subjects are shown in Figs. 7–9. These figures indicate comparisons of the measured temperatures with the predicted temperatures obtained by using the estimated values. It can be found that the predicted temperature curves obtained by the parameter estimation method are basically in agreement with the measured temperatures. However, it is obvious that the measured temperatures match the predicted temperatures well at the heating stage, but do not match as well at the cooling stage. On the one hand, this is due to the existence of the intrinsic difference between the actual heat-transfer process of the human forearm and the established mathematical model.

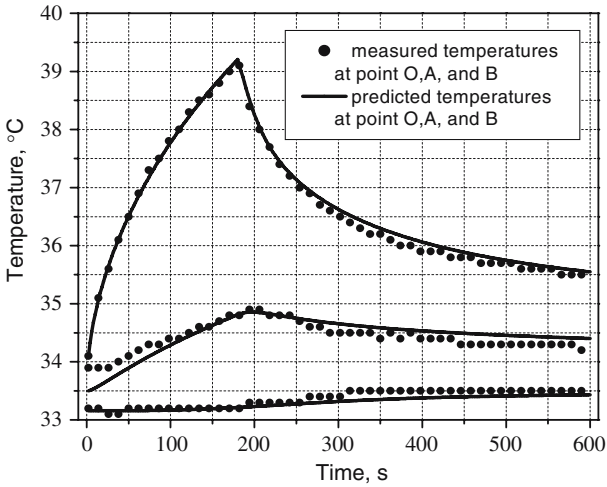

Fig. 7. Measurement results for subject 1.

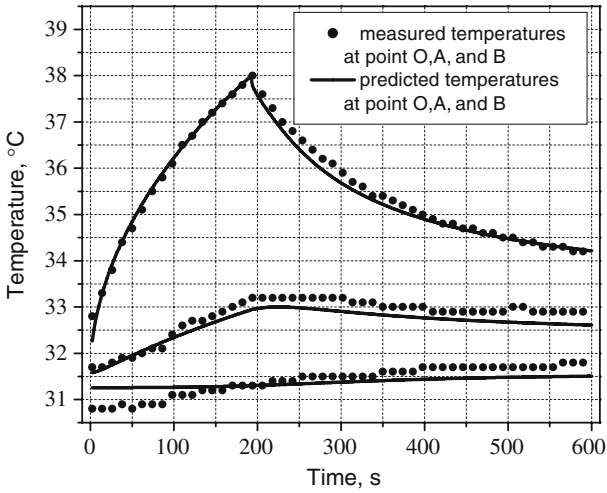

Fig. 8. Measurement results for subject 2.

On the other hand, it is possible that the external heat flux does not immediately change to zero when the power supply is turned off, which may be caused by the effect of the heat capacity of the sheet metal. This point requires further investigation of possible modifications to the value of the heat flux.

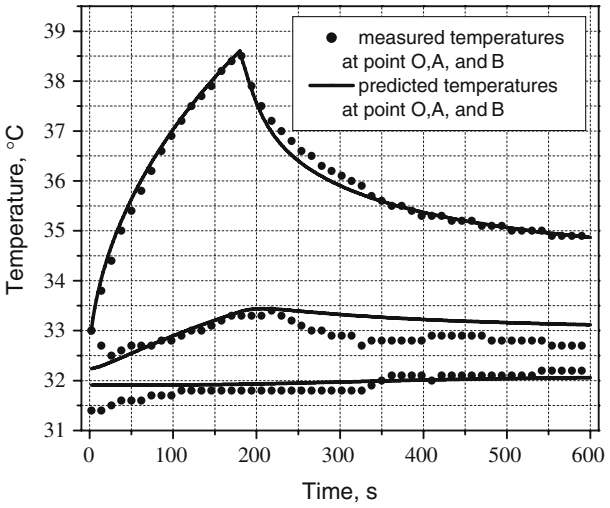

Fig. 9. Measurement results for subject 3.

In addition, the simultaneous estimations of four parameters, k, w_b, ρc, and h_A, have been performed for the case where the objective function (S_O) is defined as the function of the data from only measuring point O. One of the experimental results shown in Fig. 10 indicates that the measured temperatures at the point O match well with the predicted temperatures while the measured temperatures at points A and B differ greatly from the predicted temperatures at the same sites. This result suggests that the estimation errors of simultaneous measurement of multiple parameters are large when the temperature data of only one measuring point is used. For each subject, the same experimental procedures have been repeated three times under the same experimental conditions. The results are illustrated in Table VII. The optimal estimated value of the thermal parameter is expressed as the average of the results of three experiments along with the absolute error of replication.

Referring to existing data of published papers, we can conclude that the thermal parameters obtained in this paper, such as the thermal conductivity, blood perfusion, and volumetric heat capacity, are within the reasonable parameter ranges of living tissue. However, the obtained errors of replication are greater than expected. In future work, optimal design and implementation of the experiments deserve further investigation.

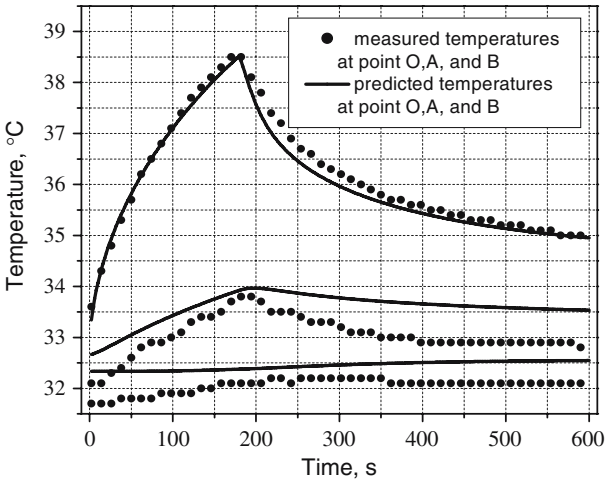

Fig. 10. Measurement results obtained by using the objective function S_O.

Table VII. Results of Thermal Parameter Measurements of Human Forearms

	Subject	Estimated value
1	k $(W \cdot m^{-1} \cdot {}^{\circ}C^{-1})$	0.62 ± 0.02
	w_b $(kg \cdot s^{-1} \cdot m^{-3})$	0.37 ± 0.03
	ρc $(J \cdot m^{-3} \cdot {}^{\circ}C^{-1})$	$2.92 \times 10^6 \pm 0.09 \times 10^6$
2	k $(W \cdot m^{-1} \cdot {}^{\circ}C^{-1})$	0.46 ± 0.04
	w_b $(kg \cdot s^{-1} \cdot m^{-3})$	0.67 ± 0.03
	ρc $(J \cdot m^{-3} \cdot {}^{\circ}C^{-1})$	$3.32 \times 10^6 \pm 0.19 \times 10^6$
3	k $(W \cdot m^{-1} \cdot {}^{\circ}C^{-1})$	0.57 ± 0.03
	w_b $(kg \cdot s^{-1} \cdot m^{-3})$	0.43 ± 0.03
	ρc $(J \cdot m^{-3} \cdot {}^{\circ}C^{-1})$	$3.33 \times 10^6 \pm 0.21 \times 10^6$

5. CONCLUSION

In order to simultaneously measure the key thermal parameters of the cylindrical living tissue, the temperature variations of three measuring points on the surface of the body are measured for the case where the external heat perturbation signal is applied and then removed. The corresponding mathematical model is set up and is calculated numerically to obtain predicted temperature variations. Using the designed real-coded GA, the measured parameters are estimated by minimizing the objective function. The simulation results indicate that five parameters involved in the mathematical model cannot be simultaneously estimated with good

accuracy. Therefore, the simultaneous estimations of three or four parameters are simulated and experimentally studied.

The simulation and experimental results show that the new method is feasible and effective to simultaneously measure thermal parameters of cylindrical living tissue and can provide valuable information for the development of a noninvasive measurement technique. Further research is desirable to optimize the design of the practical experiments to reduce the errors replication of the measured parameters.

NOMENCLATURE

c	specific heat
h	heat transfer coefficient
k	thermal conductivity
L	cylinder length
l	heater length
q	heat flux
r	cylinder radius
S	least-squares function
T	temperature
t	time
w	blood perfusion
Greek symbols	
β	parameter
ρ	density
Subscripts	
a	artery
b	blood
c	core
t	tissue
w	water
m	metabolism
v	vein
s	surface
∞	at infinity

ACKNOWLEDGMENTS

The authors appreciate the support of "Cross-Century Talents Projects of Educational Ministry of China" and the National Natural Science Foundation of China (No. 50546029).

REFERENCES

1. K. R. Diller and T. P. Ryan, *ASME J. Heat Transfer* **120**:810 (1998).
2. J. Liu and C. C. Wang, *Bioheat Transfer* (Science Press, Beijing, 1997), (in Chinese).
3. J. C Chato, ed., *Thermal Problems in Biotechnique* (ASME Symp. Ser., New York, 1968).
4. H. F. Bowman, E. G. Cravalho, and M. Woods, *Ann. Rev. Biophys. Bioeng.* **4**:43 (1975).
5. H. Arkin, K. R. Holmes, and M. M. Chen, *ASME J. Biomech. Eng.* **111**:27 (1989).
6. D. Wei, G. M. Saidel, and S. C. Jones, *IEEE Trans. Biomed. Eng.* **137**:1159 (1990).
7. P. A. Patel, J. W. Valvano, and J. A. Pearce, *ASME J. Biomech. Eng.* **109**:330 (1987).
8. C. Naresh, H. Cao, Y. Y. David, and J. W. Valvano, *IEEE Trans. Biomed. Eng.* **48**:261 (2001).
9. E. P. Scott, P. S. Robinson, and T. E. Diller, *Meas. Sci. Technol.* **9**:889 (1998).
10. T. B. Reilly, T. L. Gonzales, and T. E. Diller, *ASME J. Biomech. Eng.* **34**:67 (1998).
11. Z. S. Deng and J. Liu, *Chin. J. Biomed. Eng.* **20**:607 (2001) (in Chinese).
12. J. W. Valvano, J. T. Allen, and H. F. Bowman, *ASME J. Biomech. Eng.* **106**:193 (1984).
13. E. H. Wissler, *J. Appl. Physiol.* **55**:35 (1998).
14. H. H. Pennes, *J. Appl. Physiol.* **1**:93 (1948).
15. J. A. J. Stolwijk, *A Mathematical Model of Physiological Temperature Regulation in Man* (NASA, CR1, 1971) .
16. K. Yue, X. X. Zhang, and F. Yu, *J. Beijing Sci. Technol.* **13**:255 (2004) (in Chinese).
17. J. V. Beck and K. J. Arnold, *Parameter Estimation in Engineering and Science* (John Wiley and Sons, New York, 1997).
18. K. Deb, A. Anand, and D. Joshi, *Evol. Comput.* **10**:345 (2002).
19. S. Tsutsui and D. E. Goldberg, *Inform. Sci.* **133**:229 (2001).